Asymmetric long-range hybrid-plasmonic modes in asymmetric nanometer-scale structures

Wen Ma and Amr S. Helmy*

The Edward S. Rogers Sr. Department of Electrical and Computer Engineering, University of Toronto, 10 King's College Road, Toronto, Ontario M5S 3G4, Canada
**Corresponding author: a.helmy@utoronto.ca*

Received March 11, 2014; revised May 16, 2014; accepted May 17, 2014;
posted June 2, 2014 (Doc. ID 207936); published June 30, 2014

The structural symmetry required for long-range surface-plasmon-polariton modes to take place is examined and mapped to asymmetric plasmonic structures. This study leads to a design methodology that facilitates the realization through systematic design of long-range modes in any asymmetric hybrid plasmonic waveguide (AHPW). Examining the modal behavior of an AHPW reveals that field symmetry on either side of the metal is the only necessary condition for plasmonic structures to support long-range propagation. We report that this field symmetry condition can be satisfied irrespective of asymmetry in a waveguide structure, material, or even field profile. The structure is analyzed using the coupled mode theory, transfer matrix method, and finite-difference time-domain method. The AHPW supports high-loss antisymmetric and long-range symmetric supermodes. Dispersion of these supermodes with respect to waveguide dimensions display similar anticrossing characteristics to those obtained in two coupled harmonic oscillators, where the propagation losses display peaks and troughs in the vicinity of the anticrossing region. To place the work in perspective, an AHPW with a width of 200 nm was found to support a long-range supermode with a subwavelength mode area of 0.23 μm^2 and propagation loss of 0.025 $dB \cdot \mu m^{-1}$ at the wavelength of 1550 nm, providing a radically improved attenuation confinement trade-off compared with other common types of plasmonic waveguides.

OCIS codes: (230.0230) Optical devices; (230.7370) Waveguides; (240.6680) Surface plasmons; (250.3140) Integrated optoelectronic circuits.
http://dx.doi.org/10.1364/JOSAB.31.001723

1. INTRODUCTION

Surface plasmon polaritons (SPP) are quasi-two-dimensional (2D) surface electromagnetic waves that propagate along dielectric–metal interfaces with field components decaying exponentially into both media [1]. Field penetration into the dielectric typically ranges between hundreds to thousands of nanometers, while confinement in the metal is limited to tens of nanometers and is determined by its skin depth [2]. These attributes have inspired significant research effort, which is pertinent to nanoscale plasmonic effects and devices for applications, such as subwavelength focusing, waveguiding, modulation, sensing, and spectroscopy. Recent progress in this field has been summarized in several review articles [3–5]. One of the prominent properties of plasmonics has to do with the complex permittivity of metals in the optical frequency regime, which results in small skin depths and significant absorption losses. This leads to a trade-off between the propagation length and modal field confinement factor. This severely limits the advantages, applicability, and performance of plasmonic devices.

Many techniques and design methodologies have been proposed and deployed to reduce losses in plasmonic waveguides. These can be categorized into two branches: one branch attempts to use a gain medium to compensate for the losses. This method is impractical due the high current densities involved and large waveguide dimensions required [6]. The other branch reduces the attenuation by reducing the mode field overlap with the metal at the cost of reducing the field confinement. Examples of this approach include the long-range SPP (LRSPP) strip waveguides [7], dielectric-loaded plasmonic waveguides [8], and hybrid plasmonic waveguides (HPW) [9]. Among these structures, the LRSPP waveguide has achieved the lowest propagation loss. However, this comes at the cost of larger waveguide dimensions with micrometer-scale mode areas, which are often larger than those of single-mode dielectric waveguides [7]. Moreover, the strict structural symmetry requirements that are essential for maintaining the low-loss condition severely limit the dimensions and applicability of these devices. Recently, multilayered structures also have been proposed to obtain long-range modes [10,11] based on HPW. Although these structures provide stronger confinement with reasonable loss, theoretical [12,13] and experimental [14] studies have demonstrated that strict structural symmetry is still critical for preserving the low-loss nature and avoiding modal cut-off [15]. To the best of our knowledge, there has been no in-depth analysis on the exact nature of the symmetry required to excite long-range modes in asymmetric structures.

In this work, we examine in-depth the factors necessary for a plasmonic waveguide to be able to support long-range modes. This in turn leads to a novel design methodology to obtain long-range modes in any asymmetric hybrid plasmonic waveguide (AHPW) [16]. Adopting a novel coupled waveguide approach in the closed-form analysis, this study demonstrates that it is the field symmetry (field orthogonal to the layers' interfaces) on either side of the metal that is required to

achieve long-range modes, with no need for structural or even mode symmetry. This field symmetry by the metal layer can in turn be engineered in highly asymmetric structures, irrespective of the materials and dimensions used. The findings provide a systematic approach, which makes it possible, to our knowledge for the first time, to obtain long-range modes in highly asymmetric waveguides while maintaining subwavelength dimensions and subwavelength field confinement.

2. COUPLED WAVEGUIDE APPROACH FOR STUDYING FIELD SYMMETRY REQUIREMENTS

To examine the condition necessary for supporting long-range modes, the characteristics of a five-layer AHPW will be investigated (Fig. 1) as an example, but the results can be applied to any other structure. The AHPW consists of a metal film (ϵ_4) as the middle layer with low-index (ϵ_3 and ϵ_5) and high-index (ϵ_2 and ϵ_6) dielectric layers on each side. The structure can be considered as two sections: a top HPW (HPW1) and a bottom HPW (HPW2). The two sections form a coupled mode system when the metal layer is sufficiently thin. The dispersion properties of this structure with respect to the various design parameters will be investigated. This assists in offering physical insight regarding the role that the field distribution and the symmetry of the entire structure play in determining the field confinement-loss trade-off.

This multilayer structure supports two relevant tenets, which have been proven in previous work to reduce the propagation loss of SPP modes [9,7]: (1) in HPW, propagation loss can be reduced by adding a low-index dielectric layer adjacent to the metal layer to decrease field penetration into the metal [9]. Since the field penetration into the dielectric is the dominant factor in determining the modal extent, confinement in the dielectric is increased through the presence of another high-index dielectric layer [9]. (2) The coupling of two interface plasmon waves across a metal can result in the formation of a symmetric supermode, which has smaller propagation loss when compared with single interface SPP waves guided by the same metal and dielectric material [7]. The AHPW studied in this work builds on these two principles to achieve hybrid plasmonic modes, which have an asymmetric profile with an unprecedented low loss in asymmetric structures.

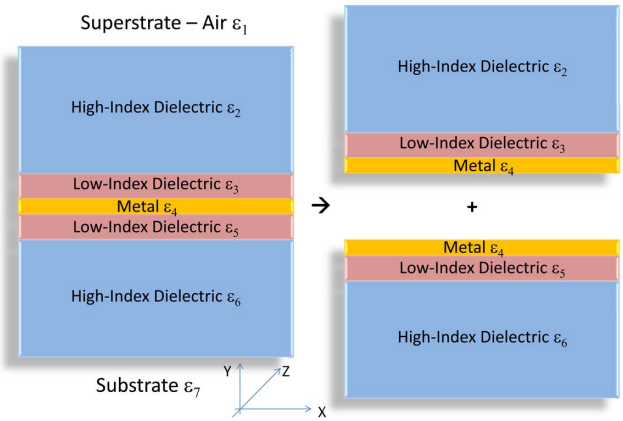

Fig. 1. Schematics of the asymmetric hybrid plasmonic waveguide. When the metal film with ϵ_4 is sufficiently thick, the system can be seen as two decoupled hybrid plasmonic waveguides, HPW1 and HPW2.

Waveguides with a similar cross section to AHPW have been proposed as candidates for hybrid plasmonic modes [10,11]. However, similar to the LRSPP work, these waveguides achieve field symmetry through structural symmetry in order to support long-range modes, i.e., the thicknesses and materials of the low-index dielectric layers must be the same ($\epsilon_3 = \epsilon_5$) and similar for the high-index dielectric layers ($\epsilon_2 = \epsilon_6$). Furthermore, to ensure that modal fields are not affected by the refractive index difference between the cladding and substrate, the thickness of the high-index dielectric layers needs to be extended [10] or additional dielectric layers should be included [11]. This dictates that the modal fields must not be affected by the refractive index difference between the cladding (air) and the substrate (ϵ_7), which is achieved by increasing the high-index dielectric layer thicknesses [10] or through adding additional dielectric layers [11]. This results in micrometer-scale waveguide dimensions, which are impractical for nanoscale device design. Moreover, the stringent material symmetry requirement not only limits the material platforms that can be used, but is also easily compromised during practical implementations due to unavoidable fabrication tolerances. Thus a different approach is needed to achieve long-range modes, while maintaining the advantages of HPW.

The AHPW structure allows the two nearly independent waveguides (HPW1 and HPW2) to be dissimilar. This means that the natural structural/material asymmetry brought about due to the refractive index difference between the top cladding and the substrate can be tolerated without having an impact on the low-loss condition. The distinct advantage of our two coupled waveguide approach and the associated structure is that the various layers in the structure are utilized to provide extra degrees of freedom to manipulate and render the field distribution symmetric across the metal layer. This is achieved without having the mode itself or the structure fully symmetric as required in all the previous work.

To demonstrate the hypothesis of achieving field symmetry across the metal layer in asymmetric structures, a waveguide will be designed as per the form shown in Fig. 1. Specifically, in this work, the wavelength of operation is selected to be 1550 nm, and only the thickness of the top high-index dielectric layer (ϵ_2) will be changed to manipulate field symmetry. The thicknesses of the other layers, ϵ_3, ϵ_4, ϵ_5, and ϵ_6, will be 20, 20, 50, and 220 nm, respectively. The high-index dielectric, low-index dielectric, and metal layers are chosen to be Si ($\epsilon_2 = \epsilon_6 = 12.11$), SiO_2 ($\epsilon_3 = \epsilon_5 = 2.07$), and Al ($\epsilon_4 = -252.5+$ i46.07), respectively [17]. It is important to highlight that these choices were made to suit practical device implementations. Any other combination of layers can be used to engineer field symmetry. There is no restriction on material properties or symmetry; thus the waveguide can be designed with great flexibility to suit a wide range of application and platforms.

3. MODE ATTRIBUTES STUDIED ANALYTICALLY IN 1D

It is insightful to first examine modes supported by the proposed AHPW structure using 1D confinement. This will be carried out by analyzing the modes of the structures as the supermodes of the two coupled HPWs. Furthermore, additional physical intuition is gained by comparing HPW1 and HPW2 in analogy to a pair of harmonic oscillators

coupled through a middle string, which demonstrates similar properties [18].

The structures HPW1 and HPW2 support both TE and TM polarized modes. TE modes are of a total internal reflection nature and propagate primarily in the high-index Si layers. TM modes are plasmonic in nature with high field concentration in the low-index SiO_2 layers, which interfaces with the metal. For a sufficiently thin common metal layer, HPW1 acts as perturbation onto HPW2 and vice versa, resulting in coupling between the modal fields of both waveguides. This creates a set of supermodes. The equations of motion for coupled oscillators describe this perturbation as an effective force from one oscillator applied onto the other through the common string connecting the two [18]. The AHPW also supports both TE and TM supermodes. However, since the modes of the two HPWs can couple in-phase or out-of-phase, the resulting TE and TM modes can be further categorized into transverse symmetric and antisymmetric supermodes. This is similar to the two eigenfrequencies found in coupled oscillator systems with the hard mode oscillating antiphase extending and compressing the middle string and the soft mode oscillating in-phase, never altering the string tension [18]. As will be shown below, the TM symmetric supermode can be identified as the long-range mode.

The dispersion properties of the modes with respect to the ϵ_2 Si layer thickness are calculated analytically using the transfer matrix formulation as described by Chen and coworkers [19]. The TM modes guided in the AHPW, HPW1, and HPW2 structures are shown in Fig. 2. The dotted curves in Fig. 2(a) show the TM modal properties of the decoupled waveguides, HPW1 and HPW2. As the thickness of the Si (ϵ_2) layer increases, the effective mode index of HPW1 approaches that of HPW2 and eventually matches it. For a sufficiently thin ϵ_4 Al layer, the HPW1 and HPW2 become coupled to form the TM symmetric and antisymmetric supermodes, which demonstrate a characteristic anticrossing behavior similar to that of two coupled harmonic oscillators. This anticrossing is a characteristic fingerprint of coupling between the two waveguides, which increases with coupling strength. The propagation losses of AHPW, HPW1, and HPW2 with respect to the Si (ϵ_2) layer thickness are illustrated in Fig. 2(b). There are two noteworthy points to discuss: (1) at the anticrossing, the long-range symmetric supermodes displays minimum propagation loss, whereas the antisymmetric supermodes displays maximum propagation loss; (2) there is a range of thicknesses for which the symmetric mode has propagation loss that is smaller than either of the decoupled waveguides, HPW1 and HPW2. The TE supermodes exhibit similar behavior. However, they will not be discussed in detail in this report.

The symmetric supermode follows the dispersion curve for HPW1 before the anticrossing and then approaches the curve for HPW2 after the anticrossing. This behavior is also illustrated in the evolution of field distribution in Fig. 3, which shows field profiles of the symmetric and antisymmetric supermodes as the Si (ϵ_2) layer thickness increases. At the two extremities of the dispersion curve, as can be seen for the symmetric supermodes in Figs. 3(d)–3(f), the majority of the field transfers from HPW1 to HPW2. In this case, the optical field is mostly located on the side of the metal with a lower effective index. The opposite holds true for the antisymmetric supermodes, which is localized on the side of the

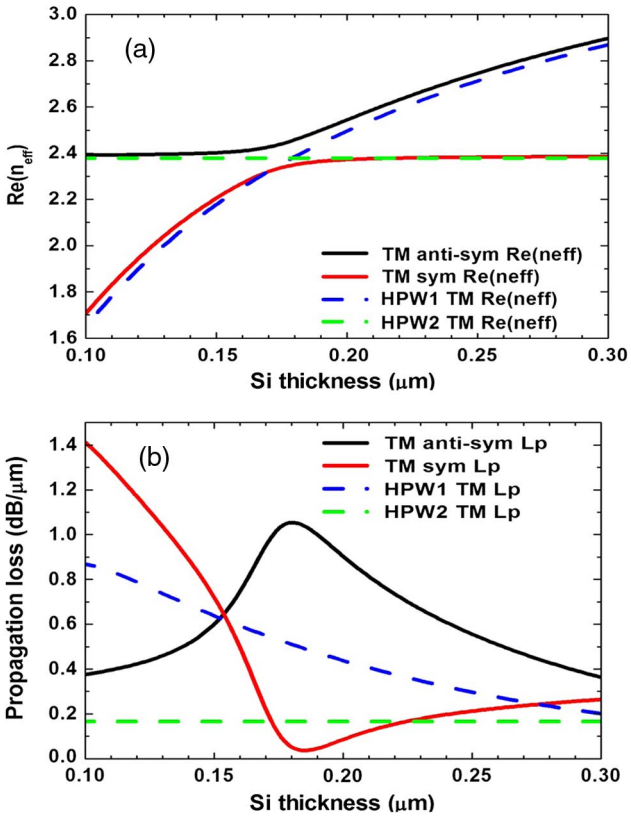

Fig. 2. (a) Effective mode index and (b) propagation loss of the AHPW, HPW1, and HPW2 with respect to the ϵ_2 Si layer thickness. The TE mode can become cut off at the dimension predetermined by the configuration of the vertical structure. Below this dimension the waveguide supports only the TM mode.

metal with a higher effective index. There is a specific Si (ϵ_2) layer thickness for which field distribution, with respect to the center of the metal, is antisymmetric-like [Fig. 3(b)] and symmetric-like [Fig. 3(e)]. These field distributions correspond to the supermodes at the anticrossing point with maximum and minimum propagation loss, respectively.

For these coupled waveguides, parallels can be drawn to a system of coupled oscillators, where analogous anticrossing characteristics are explained by the distribution coefficient, which corresponds to the field distribution in the waveguides. The eigenfrequencies of the coupled oscillator system depend on the mass and spring constant of both oscillators. By varying the mass of one oscillator, the system displays similar anticrossing: the oscillation of the system is localized in one particle, then equally engages both particles at the anticrossing, and finally restores localization in the other particle. At the point of anticrossing, the two particles are identical with the same mass [18]. This explains how one can engineer the system of coupled particles, or coupled waveguides in our case, to drive down the losses for the symmetric supermode. This design approach is in stark contrast with the work that has been carried out to date, as recent work has merely attempted to reduce the propagation losses by introducing strict structural symmetry or minimizing the overlap between the modes and the metal.

For further understanding of HPW1 and HPW2, it is insightful to use coupled mode theory (CMT) to examine the coupling strength between two waveguides. When the metal

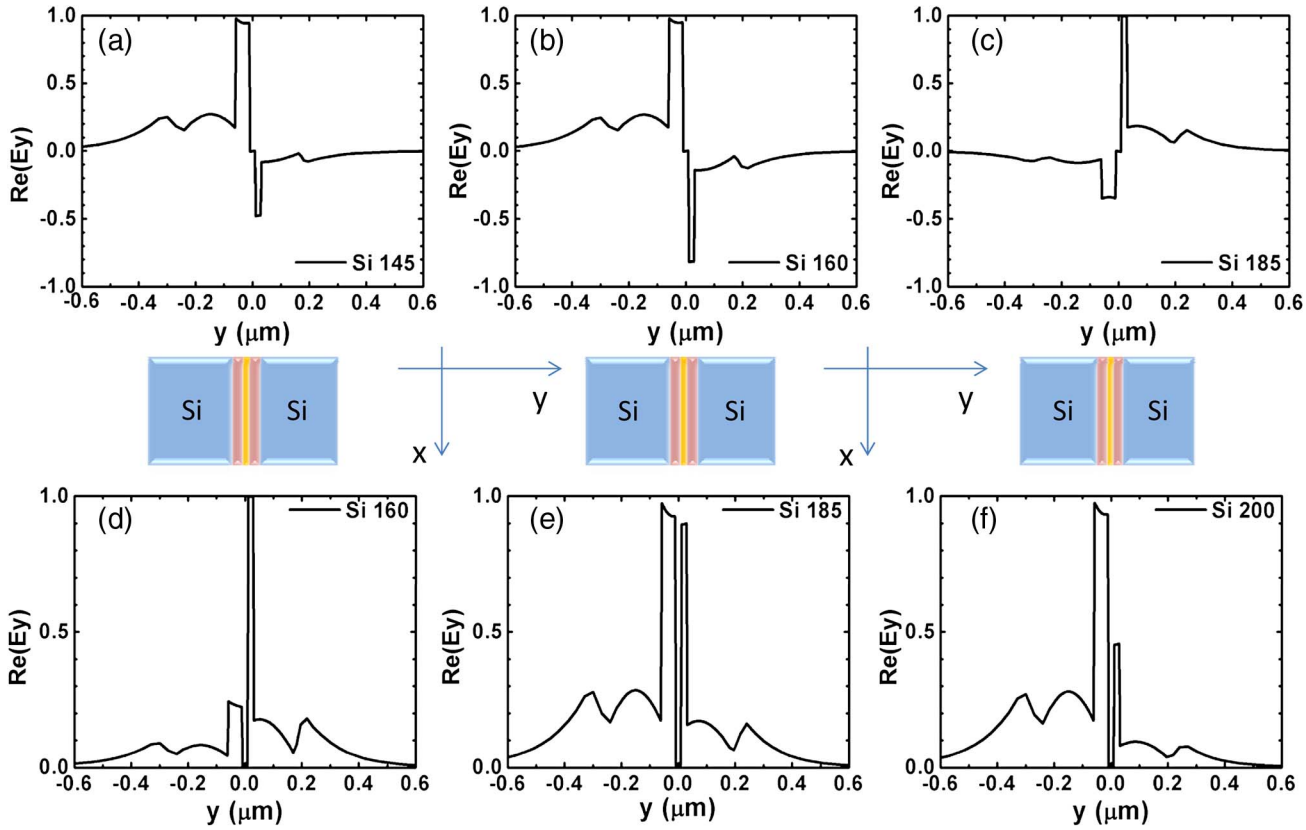

Fig. 3. Vertical transverse field profiles of the [(a)–(c)] antisymmetric supermode and the [(d)–(f)] symmetric supermode with increasing ϵ_2, which is the top Si layer thickness.

thickness is reduced to its skin depth, coupling between HPW1 and HPW2 occurs as the fields tunnel through the metal. The limiting assumptions associated with CMT are not restrictive for the structures considered here because, even though the separation between the waveguides is small, coupling is weak due to strong damping in the metal. Furthermore, HPW1 and HPW2 can be phase matched such that the effective mode index difference between HPW1 and HPW2 is small. Based on CMT, the coupling coefficient of the waveguides depend on impedance mismatch, overlap between the coupled modes, and the field perturbation from the neighboring waveguide. Using the CMT formulation by [20], which is based on the reciprocity theorem, the coupling coefficients for HPW1 and HPW2 are calculated with respect to the Si layer thickness (Fig. 4). The two waveguides are nonidentical, therefore their coupling coefficients are also dissimilar. Through varying the Si (ϵ_2) layer thickness, the difference between the two waveguides can be adjusted. In Fig. 4, it is evident how the coupling coefficients of HPW1 and HPW2 cross for both the TM and TE polarization. When

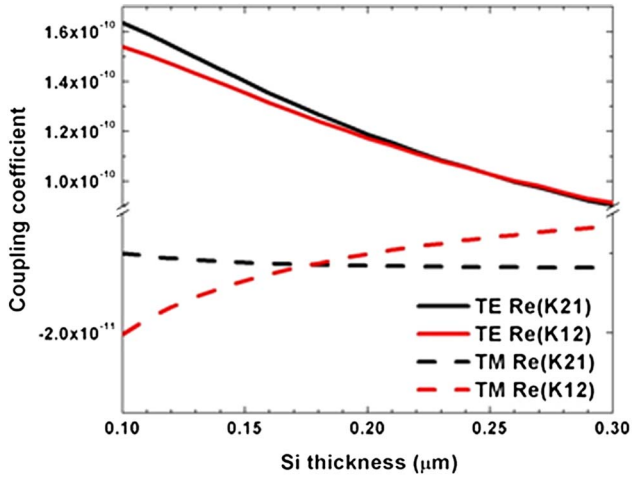

Fig. 4. Real components of the complex coupling coefficient with respect to the ϵ_2 Si layer thickness for HPW1 (κ_{12}) and HPW2 (κ_{21}) for the TE and TM modes.

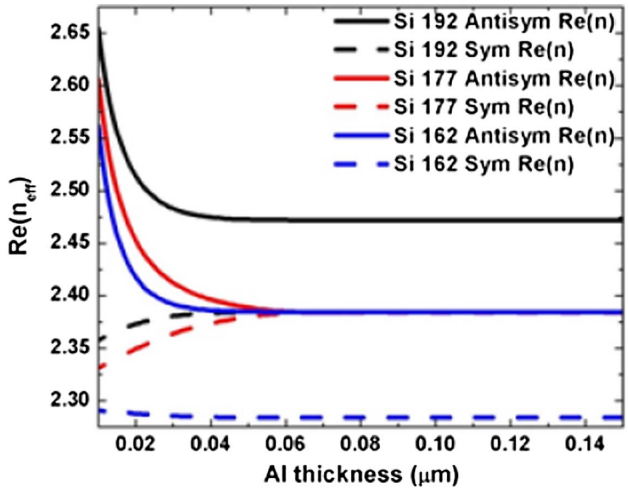

Fig. 5. Dispersion of the TM modes with respect to the metal layer thickness for an Si (ϵ_2) thickness of 192, 177, and 162 nm.

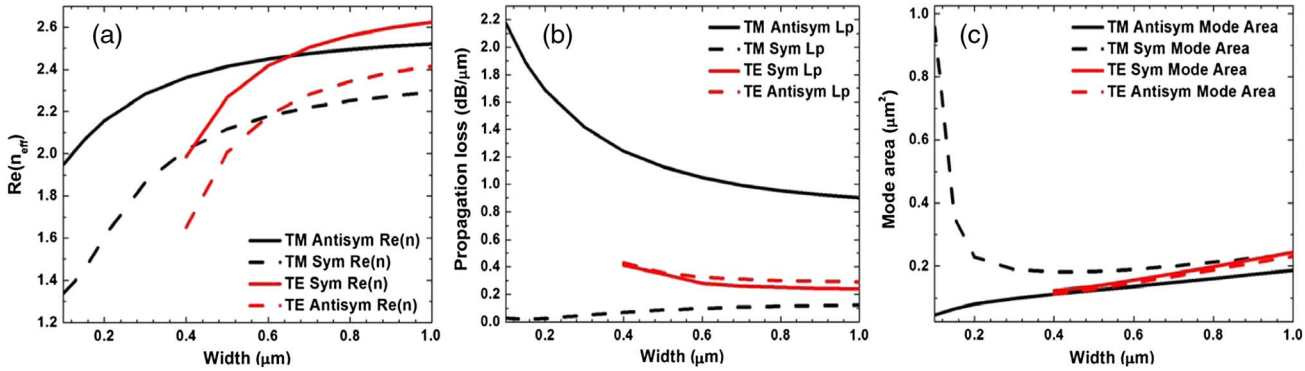

Fig. 6. (a) Effective mode index. (b) Propagation loss. (c) Mode area of guided modes in a 2D AHPW with respect to the waveguide width.

the Si (ϵ_2) thickness is 177 nm, the HWP1 and HPW2 are matched for the TM supermode and behave like two identical waveguides. The same condition is observed for the TE supermodes when the Si thickness is 246 nm.

In order to place our results in perspective, they are compared with plasmonic strip waveguides, which support LRSPP modes. In this waveguide, the metal thickness determines the coupling between its SPP modes at each interface and thus controls propagation loss and confinement [7,13]. In symmetric structures, such as a metal strip embedded in a completely homogeneous dielectric, the SPP on both sides of the metal are momentum matched; therefore the antisymmetric and symmetric supermodes become degenerate for sufficiently thick metal films for which the two SPPs become decoupled [7]. However, for asymmetric structures with a metal strip on a substrate that differs from the top cladding, the degeneracy is lifted because the SPPs on both sides of the metal are no longer matched [13]. Both of these cases can be observed for ASHW with different Si (ϵ_2) thickness, as shown in Fig. 5, which examines the dispersion as a function of Al thickness for waveguides with an Si (ϵ_2) thickness of 192, 177, and 162 nm. The Si (ϵ_2) thickness of 177 nm corresponds to the matched structure with minimum propagation loss for the TM symmetric supermode, and it is observed that the antisymmetric and symmetric supermodes for this waveguide become degenerate for thick Al thickness as in symmetric structures [7]. However, for the two other Si thicknesses, the supermodes do not become degenerate. Instead, the modes, which reside mostly in HPW1, deviate from the degenerate effective mode index. As the Al thickness increases and the two waveguides become decoupled, the mode residing in HPW2 always asymptotically approaches the same propagation constant of the fundamental mode, which is guided by HPW2.

This comparison highlights the distinctions and similarities between plasmonic strip waveguides and HPWs as coupled waveguide systems. The extra layers that exist in HPWs allow us to engineer the field components at the metal interface such that field symmetry can be induced with no need for any symmetry in the mode itself or the structure.

4. MODE BEHAVIOR EXAMINED NUMERICALLY IN PRACTICAL 2D STRUCTURES

Practical waveguide structures require 2D modal confinement by restricting the waveguide width to a finite size. The physical dimensions for which minimum propagation loss is achieved in 1D does not apply in 2D because more than one field component is present in the structure. This is where the symmetric field distribution engineered using the 1D structure breaks down. For long-range modes to take place in 2D, new dimensions need to be determined from the 2D dispersion relations to find the optimal dimensions for the top Si layer.

Figure 6 shows FDTD results for the waveguide dispersion as a function of AHPW width when the Si (ϵ_2) layer thickness is 210 nm. The propagation loss and confinement for the TM antisymmetric and symmetric supermodes follow different trends, as one increases while the other decreases with waveguide width. The TM mode size increases rapidly for widths of less than 200 nm, so there is an optimum waveguide width for single-mode operation and attractive mode properties. This width depends on the dimensions of the entire structure; therefore it can be optimized depending on the application requirements. The TE supermodes follow similar trends but become cut off below 400 nm.

In Fig. 7, the dispersion curves, with respect to the Si (ϵ_2) layer thickness for a waveguide with a width of 200 nm, show similar characteristics as those obtained for the 1D case (Fig. 2). The anticrossing between the TM antisymmetric and symmetric supermodes is still present. However, the difference between the modal properties of the two modes is

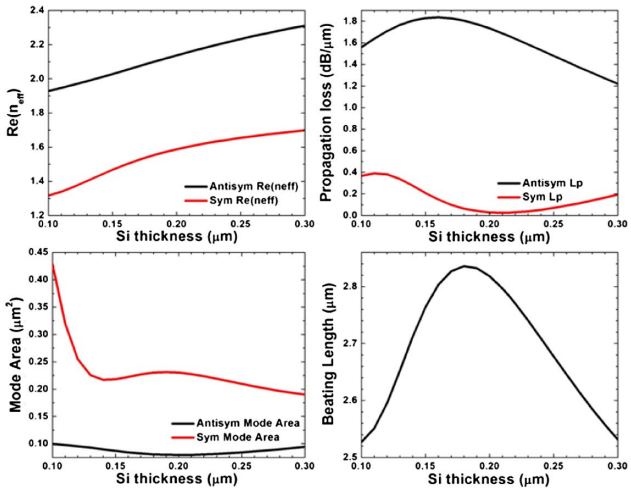

Fig. 7. (a) Effective index. (b) Propagation loss. (c) Mode area. (d) Beating length of the TM antisymmetric and symmetric modes for 2D waveguides with a width of 200 nm as a function of the Si ϵ_2 layer thickness.

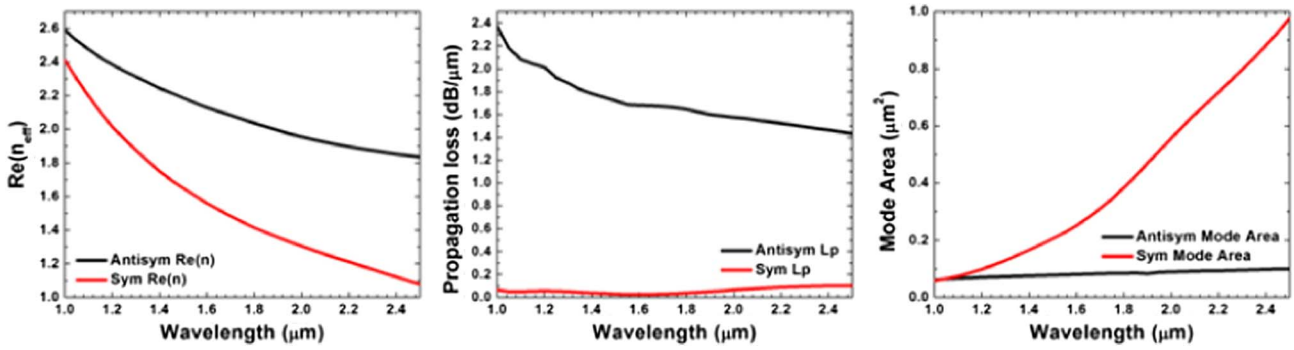

Fig. 8. (a) Effective mode index. (b) Propagation loss. (c) Mode area of guided modes in a 2D waveguide with respect to wavelength. Waveguide width is 200 nm. ϵ_2 Si layer thickness is 210 nm.

greater due to increased coupling between HPW1 and HPW2. This can be beneficial because it increases the fabrication tolerances and bandwidth of the operating regime of the long-range modes, rendering them amenable to realization using existing technologies. Furthermore, the two modes still demonstrate maximum and minimum propagation loss, which allows the waveguide to be optimized for minimum propagation losses for the long-range symmetric TM supermode. For the aforementioned waveguide dimensions, the optimal waveguide design includes an Si (ϵ_2) layer thickness of 210 nm. The TM antisymmetric supermode has an effective index of 2.16 and a propagation loss of 1.69 $dB \cdot \mu m^{-1}$, while those for the TM symmetric supermode are 1.6 and 0.025 $dB \cdot \mu m^{-1}$, respectively. This loss value for this mode area sets a new performance regime for this class of waveguides.

Dispersion of the two TM modes with respect to wavelength is rather complex because the width and thicknesses of all layers of the waveguide are changed at the same time, and they all affect the propagation constant to a varying extent, depending on the material properties. Figure 8 shows the expected behavior: as the wavelength increases, the mode fields penetrate more into the cladding, resulting in a reduced effective index, propagation loss, and field confinement. It should be noted that the waveguide is optimized for operation at 1550 nm.

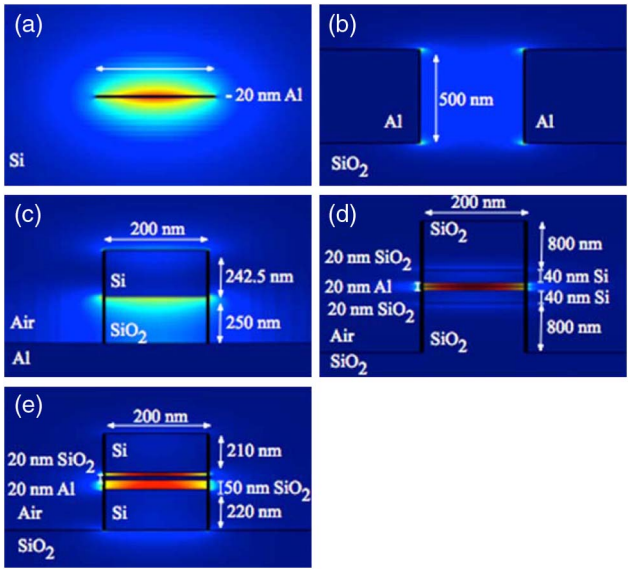

Fig. 9. Electric field profile of the following waveguides: (a) LRSPP plasmonic strip waveguide with a 20 nm × 775 nm Al strip embedded in Si. (b) Al plasmonic slot waveguide embedded in homogeneous SiO_2 with slot size of 500 nm × 220 nm. (c) Hybrid plasmonic waveguide consists of 200 nm × 250 nm SiO_2 sandwiched between 242.5 nm Si and Al film. The cladding is taken as air. (d) Symmetric hybrid plasmonic strip waveguide based on the proposed structure by [11]. From top to bottom, the structure has the following dimensions: 800 nm SiO_2, 220 nm Si, 40 nm SiO_2, 20 nm Al, 40 nm SiO_2, 220 nm Si, and 800 nm SiO_2. (e) AHPW with a width of 200 nm and (ϵ_2) Si layer thickness of 210 nm.

5. DISTINCTIONS OF THIS DESIGN APPROACH

Different plasmonic waveguides have their respective strengths and weaknesses, which can be adapted to suit various applications. However, it is instructive to compare the various plasmonic waveguides using propagation loss and field confinement. Although figures of merit have been proposed to facilitate waveguide comparison [21], parameters are often compared in regimes of dimensions where practical considerations are not taken into account. To ensure fair comparison of waveguide propagation loss, it is necessary to keep the field confinement of various waveguides, manifested in the mode area, identical. The geometries and mode profile of plasmonic waveguides under comparison are displayed in Fig. 9, and their performance attributes are listed in Table 1. It can be observed that the AHPW shows improved confinement against the LRSPP plasmonic strip waveguide and demonstrates reduced propagation loss against the Al plasmonic slot waveguide and the HPW. Although it performs similar to the hybrid plasmonic strip waveguide, its physical height is

Table 1. Comparison of Modal Properties between Designs in This Work and Previous Approaches[a]

		Propagation Loss	Mode Area
	Effective Index	in $dB \cdot \mu m^{-1}$	in μm^2
LRSPP plasmonic strip waveguide	3.49	0.025	3.5
Aluminum plasmonic slot waveguide	1.53	0.354	0.23
Hybrid plasmonic waveguide (HPW)	1.26	0.068	0.23
Hybrid plasmonic strip waveguide	1.59	0.024	0.23
Asymmetric hybrid plasmonic waveguide (AHPW)	1.6	0.025	0.23

[a]Note that the dimensions of the waveguides are chosen to provide similar mode areas for all modes to render an effective comparison of their propagation losses.

four times smaller. Overall, the AHPW has demonstrated significantly improved balance of loss and field confinement.

6. CONCLUSION

In conclusion, the nature of symmetry required for the long-range mode is established using the asymmetric hybrid plasmonic waveguide (AHPW). It has been determined that only field components across the metal are required to be symmetric for minimum propagation loss, while the mode field components within the rest of the structure can remain nonidentical. The proposed AHPW can be analyzed as two nonidentical hybrid plasmonic waveguides coupled across a common metal layer. Supermodes with symmetric and antisymmetric transverse electric field distributions are formed for both TIR modes with TE polarization, which are guided in the high-index dielectric layers, and for plasmonic modes with TM polarization, which are guided in the low-index dielectric layers. The structural asymmetry allows for nonsymmetric material composition, and, by manipulating waveguide dimensions, the field symmetry in the structure can be controlled. Dispersion of the TM symmetric and antisymmetric supermodes, with respect to the top Si layer thickness, demonstrates anticrossing that is characteristic to coupled systems.

By tuning the layers' dimensions, control over the properties of the symmetric and antisymmetric supermodes can be achieved. Thus, by engineering modal field symmetric across the metal layer, long-range propagation corresponding to the TM symmetric supermode can be obtained in any asymmetric structure, with improved field confinement. Coupled mode theory and analytical mode dispersion with respect to metal film thickness suggest that, for the matched waveguide, the structure behaves like two identical coupled waveguides, even though the physical dimensions of the two waveguides are nonidentical. We showed that AHPW with 2D confinement excite the same supermodes with similar anticrossing properties. The AHPW can be designed to have single-mode operation with the TM symmetric supermode, as the TE supermodes become cut off at small waveguide widths, and the TM antisymmetric mode experiences large propagation loss.

The AHPW has shown improved tolerance to the loss of mode confinement trade-off and reduced waveguide dimensions in comparison with the LRSPP in the plasmonic strip waveguide, the Al-based plasmonic slot waveguide, the hybrid plasmonic waveguide, and the hybrid plasmonic strip waveguide. This design approach provides a powerful tool for developing a broad range of plasmonic devices such as modulators with a small footprint and low insertion loss.

ACKNOWLEDGMENTS

The authors acknowledge support from the Natural Sciences and Engineering Research Council of Canada (NSERC) for funding.

REFERENCES

1. H. Raether, *Surface Plasmons: On Smooth and Rough Surfaces and on Gratings* (Springer-Verlag, 1988).
2. A. Dereux, T. W. Ebbesen, and W. L. Barnes, "Surface plasmon subwavelength optics," Nature **424**, 824–830 (2003).
3. S. I. Bozhevolnyi and D. K. Gramotnev, "Plasmonics beyond the diffraction limit," Nat. Photonics **4**, 83–91 (2010).
4. W. S. Cai, Y. C. Jun, J. S. White, M. L. Brongersma, J. A. Schuller, and E. S. Barnard, "Plasmonics for extreme light concentration and manipulation," Nat. Mater. **9**, 25729–25740 (2010).
5. M. I. Stockman, "Nanoplasmonics: past present and glimpse into future," Opt. Express **19**, 22029–22106 (2011).
6. G. Sun and J. B. Khurgin, "Practicality of compensating the loss in the plasmonic waveguides using semiconductor gain medium," Appl. Phys. Lett. **100**, 011105 (2012).
7. P. Berini, "Plasmon-polariton waves guided by thin lossy metal film of finite width: bound modes of symmetric structures," Phys. Rev. B **61**, 10484–10503 (2000).
8. H. Ditlbacher, A. L. Stepanov, A. Drezet, F. R. Aussenegg, A. Leitner, J. R. Krenn, B. Steinberger, and A. Hohenau, "Dielectric stripes on gold as surface plasmon waveguides," Appl. Phys. Lett. **88**, 094104 (2006).
9. J. S. Aitchison, M. Mojahedi, M. Z. Alam, and J. Meier, "Super mode propagation in low index medium," in *Conference on Lasers and Electro-Optics/Quantum Electronics and Laser Science Conference and Photonic Applications Systems Technologies*, May 2007, paper JThD112.
10. R. Adato and J. Guo, "Extended long range plasmon waves in finite thickness metal film and layered dielectric materials," Opt. Express **14**, 12409–12418 (2006).
11. G. Wang, W. Li, S. Chen, L. Xiao, D. Gao, L. Chen, and X. Li, "A silicon-based 3-D hybrid long-range plasmonic waveguide for nanophotonic integration," J. Lightwave Technol. **5**, 10742–10748 (2011).
12. R. Haupt and L. Wendler, "Long-range surface plasmon-polaritons in asymmetric layer structures," J. Appl. Phys. **59**, 3289–3291 (1986).
13. P. Berini, "Plasmon-polariton waves guides by thin lossy metal films of finite width: bound modes of asymmetric structures," Phys. Rev. B **63**, 125417 (2001).
14. N. Lahoud, G. Mattiussi, P. Berini, and R. Charbonneau, "Characterization of long-range surface-plasmon-polariton waveguides," J. Appl. Phys. **98**, 043109 (2005).
15. P. Berini and I. Breukelaari, "Long-range surface plasmon polariton mode cutoff and radiation in slab waveguides," J. Opt. Soc. Am. A **23**, 1971–1977 (2006).
16. A. S. Helmy and W. Ma, "Waveguiding in asymmetric hybrid plasmonic structures," in *IEEE Photonics Conference*, Seattle, 2013.
17. H. D. Palik, *Handbook of Optical Constants of Solids* (Academic, 1985).
18. L. Novotny, "Strong coupling, energy splitting, and level crossings: a classical perspective," Am. J. Phys. **78**, 1199–1202 (2010).
19. D. Feng, S. Tanev, V. P. Tzolov, C. Chen, and P. Berini, "Efficient and accurate numerical analysis of multilayer planar optical waveguides in lossy anisotropic media," Opt. Express **7**, 260–272 (2000).
20. S. L. Chuang, "A coupled mode formulation by reciprocity and a variational principle," J. Lightwave Technol. **14**, 1089–1091 (1987).
21. P. Berini and R. Buckley, "Figures of merit for 2D surface plasmon waveguides and application to metal stripes," Opt. Express **15**, 12174–12182 (2007).